Resistivity in the dynamic current sheath of a field reversed configuration

M. E. Kayama

Citation: Phys. Plasmas **19**, 032511 (2012); doi: 10.1063/1.3698405
View online: http://dx.doi.org/10.1063/1.3698405
View Table of Contents: http://pop.aip.org/resource/1/PHPAEN/v19/i3
Published by the AIP Publishing LLC.

Resistivity in the dynamic current sheath of a field reversed configuration

M. E. Kayama[a)]
Department of Physics and Chemistry, Sao Paulo State University, Guaratingueta, SP 12516410, Brazil

(Received 27 December 2011; accepted 7 March 2012; published online 30 March 2012)

The resistivity of a field reversed configuration in a theta-pinch with slow rising current was investigated during the turbulent phase from the moment of field reversal until end of plasma radial implosion. This transport coefficient was obtained in a hydrogen plasma by local measurements with magnetic probe and compared to numerical calculations with Chodura resistivity and evolution of lower hybrid drift instability. The values of resistivity are higher than those predicted by classical binary collision. During early phase of confinement, the doubly layer structure of current sheath in the low electric field machine was theoretically well reproduced with anomalous collision frequency calculated with Chodura resistivity that provides appropriate conditions for onset of lower hybrid drift instability and the regular evolution of pinch. The plasma dynamic, radial profiles of magnetic field during the radial compression and resistivity values were equally close to those observed by the measurements. © *2012 American Institute of Physics*. [http://dx.doi.org/10.1063/1.3698405]

I. INTRODUCTION

It is well known that transport processes in theta-pinch plasmas are dominated by turbulence. This turbulence has been associated with evolution of microinstabilities driven by various sources of free energy. On early simulations, the evolution of lower hybrid drift instability (LH) showed to be adequate to explain the smooth radial profile of the magnetic field in the current sheath during the implosion phase of theta-pinches.[1–3] Later studies have indicated that this instability is stabilized by finite beta and, therefore, should concentrate only at periphery of the current layer in a field reversed configuration (FRC).[4,5] Experimentally, no evidence of LH was observed in a FRC by CO_2 heterodyne scattering, even in low beta region at edge of configuration.[6–8] However, in a reconnection experiment, with field topology similar to FRC's, LH was observed at the edge of the current sheet by local measurements with internal electrical and magnetic probes.[9] Only this instability would not explain the fast reconnection in the device and other instabilities such as drift kink instability shows to be significant in the mechanism.[10] Recent studies shows the relevance of LH in reconnection process and FRC's.[11,12] Since its saturation level is uncertain, the use of a scaling form for particle transport rate is also suggested by other author.[13]

Resistivity is the coefficient normally used to characterize the turbulent plasmas in this field configuration. It can be evaluated using internal probe measurements and, for hot plasmas, combining non-perturbative diagnostics with numerical calculations.[14–16] The values are usually higher than predicted by Spitzer formula based in fully ionized plasma in strong magnetic field.[17] Particularly for FRC, two formulations have been used in numerical calculation of this anomalous resistivity: the Chodura resistivity and the other derived from Ohm's law and Maxwell equations sometimes written in scaling form.[18–22] They have been successfully used to describe flux losses and equilibrium in this configuration.

The present work reports the resistivity estimation in a field reversed configuration produced in a theta-pinch device. For a wide range of initial hydrogen gas pressure, this parameter was calculated from internal magnetic probe signals and numerical simulation in a numerical code where ions are taken as particle and electron as massless fluid. The analysis extended from the initial reversed field phase until the end of radial implosion phase. Two approaches were used to calculate anomalous collision frequency: the first one based on evolution of microinstabilities and the second the Chodura resistivity. Microinstabilites could not reproduce numerically the actual plasma dynamic. That was feasible combining these two methods to calculate anomalous resistivity.

In FRC, the resistivity can be derived from Ohm's law $\mathbf{E} = \eta\mathbf{J} + \mathbf{v} \times \mathbf{B}$ that reduces to $\mathbf{E} = \eta\mathbf{J}$ on magnetic axis ($\mathbf{B} = 0$) at $r = R$.[15,19,23] Since $\mathbf{B} = B\hat{\mathbf{e}}_z$ and $\mathbf{J} = J\hat{\mathbf{e}}_\theta$ in this configuration, using Faraday's and Ampere's law we obtain

$$\frac{d\phi}{dt} = -\frac{2\pi R}{\mu_0}\left(\eta\frac{dB}{dr}\right)_{r=R}, \tag{1}$$

where $\phi = -\int_0^R B2\pi r dr$. Internal magnetic probe is the obvious diagnostic technique to measure this spatial and temporal variation of the magnetic field if perturbations can be reduced. This perturbation arises from the presence of conductor in the plasma, and most seriously, the contamination and local plasma properties variation due to material produced by plasma-surface interaction. In the present experiment, plasma lasts for 1 to 2 μs with density and temperature $\sim 10^{16}$ cm^{-3} and 15 eV, respectively. Using quartz as probe jacket, the belief time of the probe, taken as the time required to evaporate material from the surface, is around 10 μs, higher than plasma existence.[24] Precaution to perturbation due finite conductivity of probe material in the plasma was done reducing probe size in proportion of 1/70 of plasma dimension.

[a)]Electronic mail: mkayama@uol.com.br.

II. NUMERICAL SIMULATION

The numerical code used is a version of $1\frac{1}{2}$ dimension (space-time, *r-t*) hybrid code AURORA with inclusion of an electron impact ionization model. The model assumes two bound states $n=1$ and $n=2$ and the continuum ($n \geq 3$) with collisional excitation and collisional de-excitation between bound states. Between bound states and continuum, the process is collisional ionization and radiative recombination.[25–27] Ions are taken as particles distributed initially in simulation grid according to a Maxwellian and electrons as a massless fluid. The massless electrons assumption excludes the possibility of LH fluctuations since LH is proportional to $1/\sqrt{m_e}$. The electron effects are expressed in terms of a anomalous electron-ion collision frequency. The Vlasov equation is solved to calculate evolution of ion distribution function $f_i(r,w,t)$. The equation of motion of each species is

$$m_i \frac{d\mathbf{w}}{dt} = e\mathbf{E} + \frac{\mathbf{w}\times\mathbf{B}}{\mu_0 c} - \mathbf{P}, \tag{2}$$

$$m_e n_e \frac{d\mathbf{v}_e}{dt} = 0 = -en_e\left(\mathbf{E} + \frac{\mathbf{w}\times\mathbf{B}}{\mu_0 c}\right) - \nabla p_e - n_e\mathbf{P}, \tag{3}$$

where $n_i = \int f_i(r,w,t)d^3w$, $\mathbf{v}_i = (1/n_i)\int \mathbf{w}_i f_i(r,w,t)d^3w$, $\mathbf{P} = e\tilde{\eta}\mathbf{J}$ is the momentum transferred from ions to the electrons per ion per unit of time due to collisions and $\tilde{\eta}$ is the resistive tensor calculated according to $\eta = m_e\nu/ne^2, \nu$ is the (anomalous) collision frequency, and $p_e = n_e kT_e$ is the pressure. Field equations are Maxwell's equations without displacement current term. Two approaches were used for collision frequency ν. The first one was the empirical Chodura collision frequency given by[18]

$$\nu_{\perp,\parallel} = c_{\perp,\parallel}\omega_{pi}[1 - \exp(-|V_{d\perp,d\parallel}|/f_{\perp,\parallel}c_s)], \tag{4}$$

where $c_s = (\gamma kT_e/m_i)^{1/2}, V_d$ is the drift velocity, and c and f are adjusting parameters. The second one accounts the evolution of three microinstabilities: Buneman two-stream, ion acoustic, and LH. Only the latter showed to be relevant to reproduce the actual theta-pinch dynamic. Its growth rate ($V_d > c_s$) is given by

$$\gamma_{LH} = \frac{\omega_{pi}}{\sqrt{1+\omega_{pe}^2/\omega_{ce}^2}}\exp(v_s/V_d), \tag{5}$$

with saturation level $\varepsilon_{LH} = 0.01 n_i m_i V_d^2/(1+\omega_{pe}^2/\omega_{ce}^2)$.
The simulation condition was based on the first strong pinch of the experiment that occurs on the third half-cycle of external current. Initial ionization fraction of gas $\alpha = n_e/n_0$ was varied in the range of 0.15–0.9, with uniform ionization or according to $\alpha\exp(-r/c_i)^2$, where c_i is a adjusting coefficient. The latter with $c_i = 3.5$ and r in the range of 0–3.7 was used in order to reproduce experimental lift-off time of current sheath. The number of particles was 5000 particles and simulation time step 5 ns. The current in the simulation coil evolves according to under damped RLC circuit with no coupling between circuit and plasma according to low coupling found in the experiment.

The evolution of plasma implosion was well reproduced in the simulation combining Chodura and LH calculations for anomalous collision frequency. The first reproduces the multi-structured current sheath of the experiment at the beginning of implosion and the latter the dynamic of the implosion. Calculations with only LH results in fast implosion with sharp current and density profile, close to zero resistivity description, different of those observed in the experiment

III. EXPERIMENT

The experiment was in a theta-pinch with 20 cm long coil and a Pyrex discharge tube with a = 3.7 cm inner radius. It operates without a crowbar, i.e., the current has a damped sinusoidal waveform with 14.7 μs rise time (quarter of period). The first pinch occurs during current rising of the third half cycle (HC) and repeats on forward HC of the discharge.[28] For the present study, we worked on the third HC where the peak magnetic field is 11 kG and azimuthal electric field at discharge wall is 76 V/cm. External magnetic probes showed no significant variation on signals with and without plasma, indicating small coupling between plasma and the discharge circuit. The reversed bias magnetic field is the field frozen to the plasma at the end of the previous HC. The intensity varies from 0.8 to 1.2 kG depending on the initial pressure of hydrogen varied in the range of 45–150 mTorr. The plasma temperature varies in the range of 10–20 eV and density $\sim 10^{16}\,\mathrm{cm}^{-3}$, calculated using pressure balance equation with assumption of mass conservation. The measurements were performed with various magnetic probes, winded in cavities of a molded epoxy structure, each probe with dimensions around 1 mm in diameter and 3 mm long. The whole set was inside a 5 mm quartz tube in radial direction in the discharge tube. A minimum of three signals on each radial position were used for analysis, with appropriate correction of amplitudes due to small variations of capacitor bank charging voltages and the delay due to the jitter on the spark-gap.

IV. RESULTS AND ANALYSIS

The code was run with various bias field intensity and showed a linear increase of lift off time with bias field in the same plasma initial condition. The initial ionization had no noticeable effect on the plasma dynamic since fully ionization is rapidly established in the current sheath. At initial times of implosion, the current sheath calculated with microinstabilities is highly conductive and its radial profile is sharply defined at null point. With Chodura resistivity with $c_\parallel = 1.2$, $c_\perp = 2.2$, $f_\parallel = 1.0$, and $f_\perp = 4.0$, this profile is broad, close to the experimental one, as shown in Fig. 1. In this figure, time is normalized to theoretical pinch time τ taken as the interval from the moment the null field point leaves the wall until the moment it reaches the minimum. The experimental value of pinch time τ_X carries more uncertainty and an estimated value of 0.1 is implicit in the normalized time t/τ_X shown in the figure. Electrons are concentrated at null field point but ions are distributed from this point until almost close to the wall. That distribution was found in all filling gas pressure of the experiment, carrying different bias field from previous half cycle of the external current. In the limit of confidence in regard to the diagnostic, no clear

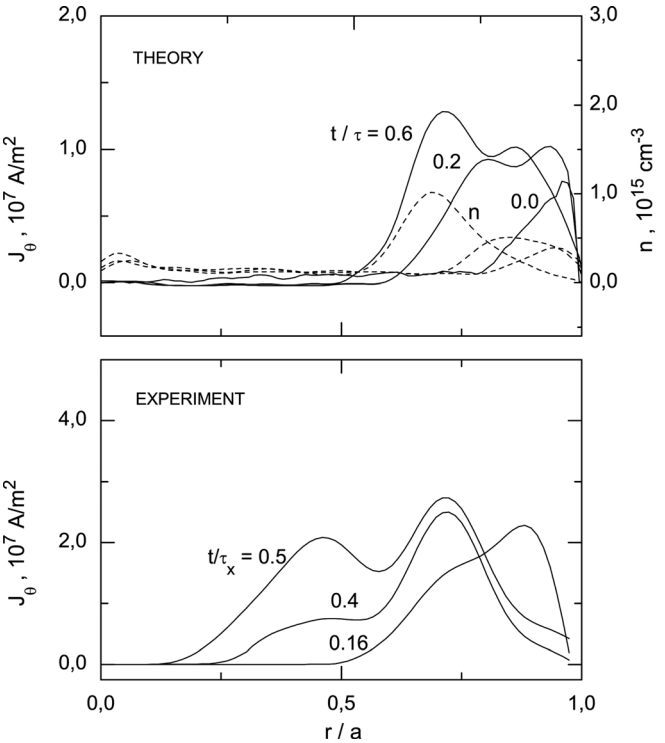

FIG. 1. Theoretical and experimental radial profiles of current density profiles (solid line) and electron density (dashed line) during early phase of radial implosion. Time is normalized to τ and τ_X, respectively, the theoretical and experimental implosion time.

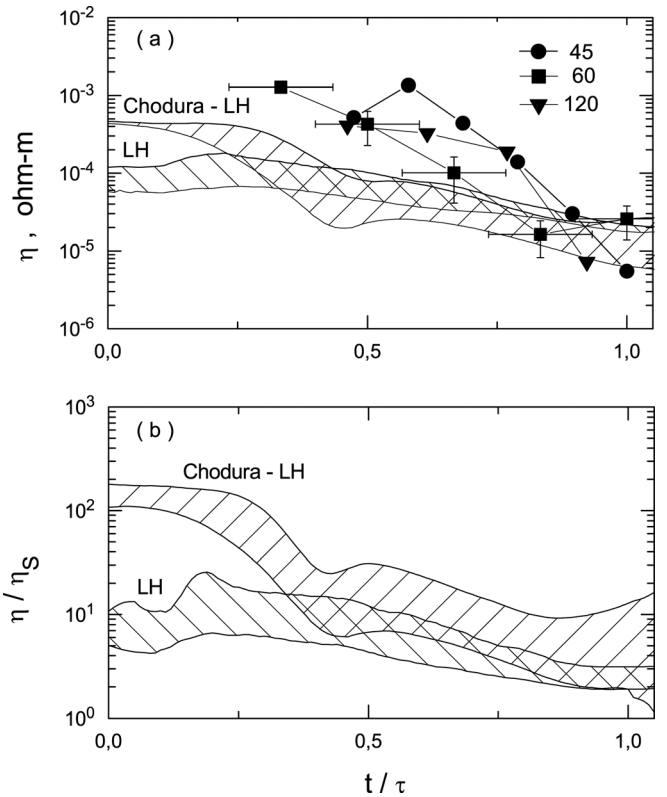

FIG. 2. Plasma resistivity at null field point during implosion phase. (a) Shaded area represents maximum and minimum calculated using LH and Chodura-LH. Experimental values are at 45/60/120 mTorr hydrogen gas pressure. (b) Correspondent maximum and minimum of resistivity normalized to Spitzer value η_S.

relation could be established among the plasma features with bias field intensity and gas pressure. A radial component of electric field evolves in the sheath pointing toward axis and presenting the same magnitude than the field in the azimuthal direction. Plasma resistivity in this phase is 100–180 times greater than classical Spitzer value and with value around 0.4 $m\Omega$ m.

A combined calculation mode was used to reproduce experimental profiles after this initial phase of implosion. Calculation starts with Chodura resistivity and changes to microinstabilities when $V_d \gtrsim 1.5c_s$ around null field point. Figure 2 shows the result of resistivity calculation using this combined method. Calculations with only LH is shown for comparison. These theoretical curves show the range between minimum and maximum values calculated from mean value and standard deviation around the null field point. The combined mode of calculation is in close agreement with experimental values. A multiplication factor in the range of 2–3 was necessary in the LH growing rate (Eq. (5)) to achieve that agreement. In the same figure, we have also the relative resistivity η/η_S normalized to Spitzer value. The resistivity value at beginning of implosion is about $\eta = (0.42 \pm 0.02)$ $m\Omega$ m and at end of implosion $\eta = (15 \pm 8)$ $\mu\Omega$ m. They correspond to $\eta/\eta_S \simeq 150$ at early phase and $\eta/\eta_S \simeq 10$ at end of implosion. On early phase, experimental resistivity is one order higher than LH calculations. At the end of implosion and beginning of the equilibrium phase, the resistivity assumes the values predicted by LH instability calculation.

Calculations in combined mode lead also to a good reproduction of radial profile of magnetic field in the experiment. That is shown in Fig. 3, where theoretical profile are superimposed to experimental points. They correspond to the time during implosion $t/\tau = 0.6$ and at end of this process $t/\tau = 1.0$. Here, we have again the uncertainty on the experimental values of pinch time and an estimated uncertainty of 0.1 is implicit in these experimental data points. The good agreement is found on the time evolution of magnetic field profiles, with a small time lag between theory and experiment.

The corresponding evolution of the pinch of this figure is shown in diagram shown in Fig. 4. After the lift off from the wall until the end of implosion, the resistive plasma remain distributed, forming a broad current profile. Behind the magnetic piston, a small amount of ions remains with

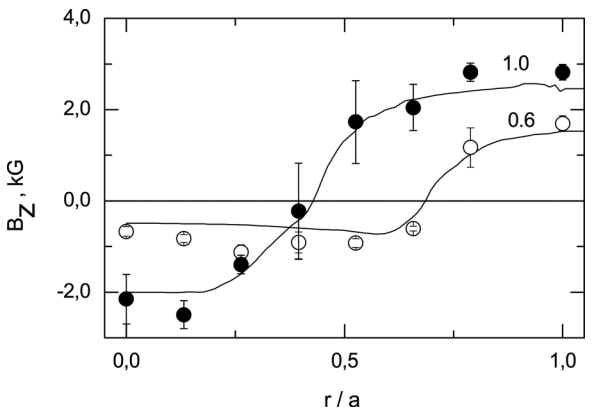

FIG. 3. Theoretical radial profile of axial component of magnetic field and experimental points at $t/\tau = 0.6$ and $t/\tau = 1.0$ with $\tau = 0.50$ μs.

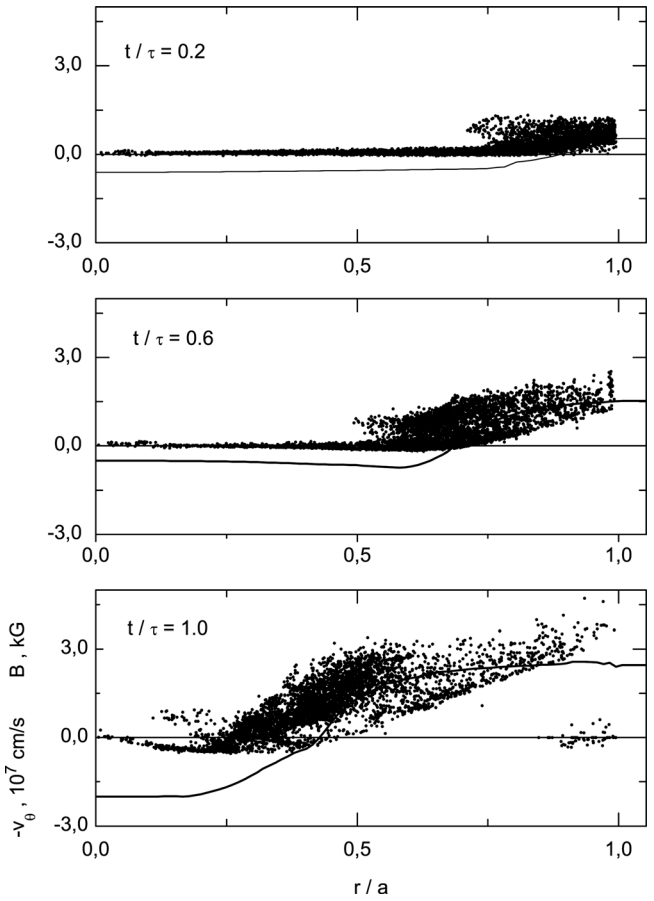

FIG. 4. $v_\theta - r$ ion phase space superposed to the profile of axial component of magnetic field during different times t/τ of radial compression.

higher speed. A electric field in radial direction is formed between electron species at the front and ions at back of piston with intensity comparable to the electric field in azimuthal direction.

V. CONCLUSION

The implosion phase of a slow rising reversed field theta-pinch was investigated with magnetic probe measurements and $1\frac{1}{2}$-D computer simulation of a hybrid code. The initial bias field intensity was between 0.8 and 1.2 kG in hydrogen plasma generated with gas pressure between 45 and 150 mTorr. The experimental plasma dynamic was well reproduced with simulation where anomalous collision frequency was calculated using initially Chodura resistivity and LH after the instant that drift speed is slightly higher than acoustic speed. Calculation of resistivity with the algorithm showed to be adequate to reproduce the experimental observations of current density radial profile with electron at front region of magnetic piston and ion species at its back forming two distinct peaks on the profile. The theoretical calculation of anomalous resistivity values using this combined mode was close to those obtained from analysis of magnetic probe measurements. Resistivity starts with high values at the beginning of implosion and reduces during the implosion. The radial profiles of the magnetic field was also in close agreement to the experiment when this combined mode to calculate the resistivity was used in the simulation.

ACKNOWLEDGMENTS

The author thanks Marcelo S. Dobrowolsky for his help in data acquisition, Paulo H. Sakanaka for supplying the computation code, and J. B. Galhardo for technical support in the machine. A special thanks to Roberto Clemente, in memoriam, for useful discussions and suggestion to this work during his existence with us. This work was supported by FUNDUNESP (Fundação de Desenvolvimento da Universidade Estadual Paulista), Contract No. 00492/08-DFP.

[1]R. C. Davidson and N. T. Gladd, Phys. Fluids **18**, 1327 (1975).
[2]P. C. Liewer and N. A. Krall, Phys. Fluids **16**, 1953 (1973).
[3]R. J. Comisso and H. R. Griem, Phys. Fluids **20**, 44 (1977).
[4]R. C. Davidson, N. T. Gladd, C. S. Wu, and J. D. Huba, Phys. Fluids **20**, 301 (1977).
[5]M. Ozaki, T. Sato, R. Horiuchi, and C. S. Group, Phys. Plasmas **3**, 2265 (1996).
[6]A. W. Carlson, Phys. Fluids **30**, 1497 (1987).
[7]J. T. Slough, A. L. Hoffman, and R. D. Milroy, Phys. Fluids B **1**, 840 (1989).
[8]S. Okada, S. Ueki, and S. Goto, Trans. Fusion Technol. **27**, 341 (1995).
[9]T. A. Carter, H. Ji, F. Trintchouk, M. Yamada, and R. M. Kulsrud, Phys. Rev. Lett. **88**, 015001 (2002).
[10]R. Horiuchi and T. Sato, Phys. Plasmas **6**, 4565 (1999).
[11]R. Kulsrud, H. Ji, W. Fox, and M. Yamada, Phys. Plasmas **12**, 082301 (2005).
[12]A. Hakim and U. Shumlak, Phys. Plasmas **14**, 055911 (2007).
[13]L. C. Steinhauer, Phys. Plasmas **18**, 070501 (2011).
[14]S. Okada, Y. Kiso, S. Goto, and T. Ishimura, Phys. Fluids B **1**, 2422 (1989).
[15]F. Trintchouk, M. Yamada, H. Ji, R. Kulsrud, and T. A. Carter, Phys. Plasmas **10**, 319 (2003).
[16]A. L. Hoffman, H. Y. Guo, R. D. Milroy, and Z. A. Pietrzyk, Nucl. Fusion **43**, 1091 (2003).
[17]L. Spitzer, Jr., *Physics of Fully Ionized Gases*, 2nd ed. (Interscience, New York, 1963).
[18]R. D. Milroy and J. U. Brackbill, Phys. Fluids **25**, 775 (1982).
[19]A. L. Hoffman, R. D. Milroy, and L. C. Steinhauer, Appl. Phys. Lett. **41**, 31 (1982).
[20]R. D. Milroy and J. T. Slough, Phys. Fluids **30**, 3566 (1987).
[21]R. E. Chrien and S. Okada, Phys. Fluids **30**, 3574 (1987).
[22]L. A. Dorf, T. P. Intrator, T. Awe, R. Renneke, S. C. Hsu, G. A. Wurden, R. Siemon, and V. E. Semenov, J. Appl. Phys. **104**, 073304 (2008).
[23]T. Intrator, S. Y. Shang, J. H. Degnan, I. Furno, C. Grabowski, S. C. Hsu, E. L. Ruden, P. G. Sanchez, J. M. Taccetti, M. Tuszewski, W. J. Waganaar, and G. A. Wurden, Phys. Plasmas **11**, 2580 (2004).
[24]M. Keilhacker, Nucl. Fusion **4**, 287 (1964).
[25]A. G. Sgro and C. W. Nielson, Phys. Fluids **19**, 126 (1976).
[26]A. G. Sgro, Phys. Fluids **21**, 1410 (1978).
[27]D. Duchs and H. R. Griem, Phys. Fluids **9**, 1099 (1966).
[28]M. E. Kayama, R. A. Clemente, R. Y. Honda, and M. S. Dobrowolsky, IEEE Trans. Plasma Sci. **37**, 2186 (2009).